

To appear in The Astrophysical Journal

## Malmquist Bias and the Distance to the Virgo Cluster

Anthony H. Gonzalez

Dept. of Astronomy and Astrophysics, University of California at Santa Cruz, Santa Cruz, CA  
95064, Email: anthonyg@ucolick.org

S. M. Faber

UCO/Lick Observatory

Dept. of Astronomy and Astrophysics, University of California at Santa Cruz, Santa Cruz, CA  
95064, Email: faber@ucolick.org

### ABSTRACT

This paper investigates the impact of Malmquist bias on the distance to the Virgo cluster determined by the  $H_0$  Key Project using M100, and consequently on the derived value of  $H_0$ . Malmquist bias is a volume-induced statistical effect which causes the most probable distance to be different from the raw distance measured. Consideration of the bias in the distance to the Virgo cluster raises this distance and lowers the calculated value of  $H_0$ . Monte Carlo simulations of the cluster have been run for several possible distributions of spirals within the cluster and of clusters in the local universe. Simulations consistent with known information regarding the cluster and the errors of measurement result in a bias of about 6.5-8.5%. This corresponds to an unbiased distance of 17.2-17.4 Mpc and a value of  $H_0$  in the range 80-82 km s<sup>-1</sup> Mpc<sup>-1</sup>.

The problem of determining the bias to Virgo illustrates several key points regarding Malmquist bias. Essentially all conventional astronomical distance measurements are subject to this bias. In addition, the bias accumulates when an attempt is made to construct “distance ladders” from measurements which are individually biased. As will be shown in the case of Virgo, the magnitude and direction of the bias are sensitive to the spatial distribution of the parent population from which the observed object is drawn - a distribution which is often poorly known. This leads to uncertainty in the magnitude of the bias, and adds to the importance of minimizing the number of steps in “distance ladders”.

### 1. Introduction

One of the longest standing challenges in modern astronomy is determination of the value of the Hubble constant. Since Edwin Hubble first observed the relation between distance and

velocity, numerous attempts have been made to accurately determine the Hubble constant relating these quantities. A variety of methods has been applied, but, despite the extensive work, different observations continue to give values that differ in their extreme by nearly a factor of two (Kennicutt, Freedman, & Mould 1995). The  $H_0$  Key Project was designed to address this situation, its primary goal being “to provide a measure of the Hubble constant accurate to 10%” (Freedman et al. 1994). With this goal in mind, the  $H_0$  Key Project has chosen to use Cepheid observations as the cornerstone method of determining distances to target galaxies. Cepheids provide a direct method of determining distance and, with HST, allow distance measurements to galaxies as distant as the Virgo and Fornax clusters. These observations can be used both to calculate the Hubble constant directly and to calibrate secondary distance determination methods that can then be applied to more distant galaxies.

Using Cepheids, the Key Project directly determined the distance to M100 to be  $16.1 \pm 1.3$  Mpc (Ferrarese et al. 1996). To obtain a value of  $H_0$ , M100 was assumed to be at the same distance as the center of the Virgo cluster, with an estimated Gaussian uncertainty of 20% due to the extended nature of the cluster. With this assumption and using a velocity for the cluster of  $1,396 \pm 96$  km s $^{-1}$ , the Key Project data yields  $H_0 = 87 \pm 20$  km s $^{-1}$  Mpc $^{-1}$ .

The goals of this paper are to bring to light the effect which Malmquist bias can have on distance measurements such as this one and secondarily to obtain a distance to the Virgo cluster corrected for this bias. Considering bias in the distance to Virgo serves to illustrate a more general point. Raw astronomical distance estimates are rarely unbiased; virtually every measured distance needs correction for Malmquist bias due to observational uncertainty. In the case of Virgo, it will be seen that the bias should not be ignored although uncertainty in the structure of the Virgo cluster precludes a precise determination of it.

## 2. Malmquist Bias

In the literature, the term Malmquist bias has been used in different places to describe related but different effects (Willick 1991). In the classical sense, the term Malmquist bias refers to a positive bias in the luminosity of objects in magnitude limited *samples*, as originally described by Malmquist in 1924 (Malmquist 1924). However, the term is now also commonly used for a related geometric bias that arises in distance measurements (Lynden-Bell et al. 1988). Of particular concern in this paper is the “inferred distance problem” (Willick 1991). In this context, to say that a measured, raw distance is subject to Malmquist bias means that the most probable value of the true distance is not the same as the raw distance.

Malmquist bias is a statistical effect and formally can be evaluated using probability theory. The general form of the expression for the bias to a single object can be written as

$$(1 + B)D = \langle r|D \rangle = \frac{\int_0^\infty rP(r|D)dr}{\int_0^\infty P(r|D)dr} = \frac{\int_0^\infty rP(r, D)dr}{\int_0^\infty P(r, D)dr}, \quad (1)$$

where  $B$  is the bias,  $D$  is the raw distance,  $r$  is the actual distance to the object being observed,  $\langle r|D \rangle$  is the expectation value of  $r$  given  $D$ ,  $P(r|D)$  is the conditional probability of  $r$  given  $D$ , and  $P(r, D)$  is the joint probability. This joint probability  $P(r, D)$  can be rewritten as

$$P(r, D) = P(r)P(D|r) = r^2n(r)P(D|r). \quad (2)$$

The  $n(r)$  term is a distribution function describing the parent population from which the object is drawn (in our case it is the distribution of Virgo-like clusters as a function of distance), so  $r^2n(r)$  is effectively the probability of selecting an object at a given distance. Meanwhile,  $P(D|r)$  contains all information about uncertainties associated with the measurement. If the only uncertainty is a Gaussianly distributed magnitude error,  $\sigma$ , then this is of the form

$$P(D|r) \propto \exp\left(-\frac{(5 \ln(r/D))^2}{2\sigma^2(\ln 10)^2}\right). \quad (3)$$

For Virgo, there is also uncertainty in the location of M100 relative to the center of Virgo.

The result for the simple case of a constant  $n(r)$  and Gaussian magnitude error was given by Lynden-Bell et al. (1988):

$$\langle r|D \rangle = D \exp(3.5\Delta^2) \approx D(1 + 3.5\Delta^2), \quad (4)$$

for small  $\Delta$ . Here,  $\Delta = \frac{\ln 10}{5}\sigma$ , and so the bias is proportional to  $\sigma^2$ .

Unfortunately, for more complicated  $n(r)$  and  $P(D|r)$  this analysis generally results in integral expressions for which analytic solutions are not possible. In such cases numerical techniques such as Monte Carlo simulations provide an efficient means of computing the bias. In order to utilize such methods, though, it is important to have a solid understanding of the physical origin of Malmquist bias. There are three key points to keep in mind:

1. Malmquist bias is a result of *observational uncertainty*, and all uncertainties contribute to the bias. Only if a distance is measured with no uncertainty will there will be no bias.
2. Malmquist bias is a *geometric effect*. When a solid angle of sky is observed, the surface area covered by that solid angle increases with distance, so a greater spatial volume is seen at greater distance. This effect is equivalent, all other factors being equal, to giving greater weight to more distant values and hence biasing the results. This makes the error envelope non-Gaussian about the observed value, being instead skewed towards greater distances.
3. When we try to measure the distance to an object, the Malmquist bias associated with that observation is dependent on *the spatial distribution of similar objects which might also have been observed*. This means that the bias in a distance measurement cannot be determined from information about the observed object alone but must also depend on the a priori spatial distribution of the sample from which the object was drawn. As an example, consider a sample of objects which is comprised of all Galactic G stars within a given solid angle

regardless of brightness. Imagine that one star in the sample is chosen at random and the distance to this star is measured. By itself, the geometric effect would imply that it is most probable that this object is infinitely far away, since the volume seen increases with distance. We know this cannot be true, however, because the distribution of Galactic G stars does not extend to infinity. Consequently, the most probable distance to the star will lie within the Galaxy.

To summarize, Malmquist bias is a geometric effect. The three-dimensional geometry of space alone tends to make the most probable value of the true distance greater than the measured, raw distance. The parent distribution of objects, is also important. It can act to increase, mitigate, or even reverse the sign of the bias. None of this matters though unless there is error. If you know exactly where something is, then there can be no bias.

### 3. Malmquist Bias and the Virgo Cluster

So far the discussion has been rather general. Now, let us return to Virgo. To determine the bias in the distance to Virgo, it is important to carefully consider each of the factors which affect the bias. In particular, there is bias only if there is observational error. What are the sources of error in the Key Project distance measurement to Virgo? Further, the bias depends on the parent distribution of objects in space from which Virgo was selected. What is the parent distribution of “Virgo-like” clusters? For that matter, what *is* a “Virgo-like” cluster? We consider each of these items in turn.

#### 3.1. Sources of Error

There are two distinct sources of error in the Key Project distance to Virgo. One is the total magnitude error in the measured distance modulus to M100. The Key Project error budget lists this value as 0.17 magnitudes (Ferrarese et al. 1996). The other source, more subtle but ultimately more important, is the extended nature of the cluster itself. The aim is to measure the distance to the center of Virgo, but M100 is not necessarily located exactly at the center. All we have is a probability distribution for the location of M100 relative to the center. This second source of error is much harder to correct for because the structure of the Virgo cluster is neither simple nor well determined.

Much research has been devoted to understanding the structure of the Virgo cluster (Tully and Shaya 1984; Sandage, Binggeli, & Tammann 1985; Binggeli, Sandage, & Tammann 1985; Binggeli, Sandage, & Tammann 1987; Fukugita, Okamura, & Yasuda 1993; Yasuda, Fukugita, & Okamura 1996). It is known that the distribution of galaxies within the cluster is not smooth, but rather exhibits several distinct density peaks. In particular there are two prominent peaks on the

sky centered near M87 (NGC 4486) and M49 (NGC 4472). Further, the distribution of galaxies within the cluster varies with morphological type, the ellipticals being more concentrated about the two peaks than the spirals (Sandage, Binggeli, & Tammann 1985). Fortunately the cluster does appear to be regular enough to allow the angular distribution of spirals to be modeled by an exponential density profile. Shaya and Tully observed a projected angular profile of spirals in the cluster with a scale length of  $\theta = 3.1 \pm 0.5$  degrees centered on the M87 group, with which M100 is believed to be associated (Tully and Shaya 1984). A similar analysis by Binggeli, Sandage, and Tammann, which excluded galaxies below  $\delta = 9^\circ$  to avoid the M49 group, yielded a value of  $\theta = 3.3$  degrees (Binggeli, Sandage, & Tammann 1987). This is the value used in the present simulations.

The line of sight profile of the cluster is less certain. Several groups have observed that the Virgo spiral B-band Tully-Fisher relation is broader than normal (Pierce and Tully 1988; Fukugita, Okamura, & Yasuda 1993; Yasuda, Fukugita, & Okamura 1996). If this excess dispersion is due primarily to the depth of the cluster, as opposed to intrinsic scatter, this would indicate that the cluster has greater line of sight depth than width on the sky.

Insight into the depth profile of the cluster can be gained from the data of Fukugita et al. (Fukugita, Okamura, & Yasuda 1993; Yasuda, Fukugita, & Okamura 1996). These authors plot the density of spiral galaxies as a function of TF distance and postulate from this that in fact the cluster is filamentary with the major axis nearly aligned with the line of sight. However, it is not immediately clear from their data how extended Virgo is along the line of sight, as the points which they plot represent a convolution of the true depth profile of the cluster with a Gaussian magnitude error from the Tully-Fisher relation.

An attempt can be made to model this convolution and determine the effective scale of the cluster along the line of sight if a form for the density distribution is assumed. As has been noted above, the distribution of spirals projected on the sky is observed to be well fit by an exponential profile of the form  $e^{-|s|/a}$ , where  $s$  is the projected distance from the center of the cluster and  $a$  is the effective scale length. We will assume that the line of sight density distribution of the cluster can also be modeled by an exponential function, but will not assume that the line of sight scale length,  $b$ , is necessarily the same as the scale length,  $a$ , projected on the sky. These scale lengths will be used to define an ellipsoidal model for the cluster; surfaces of constant density will be described by ellipsoids with eccentricity

$$e^2 = 1 - \left( \frac{a}{b} \right)^2. \quad (5)$$

In order to model the convolution, it is necessary to know the intrinsic magnitude error associated with the Tully-Fisher relation. The dispersion of the Tully-Fisher relation for the calibration galaxies of Fukugita et al. is  $\sigma = 0.29$  mag (Yasuda, Fukugita, & Okamura 1996). If it is assumed that the intrinsic scatter in Virgo is equivalent to that of the calibration galaxies, this implies a scale length  $b = 3.5 \pm 0.5$  Mpc and a TF distance of 14.4 Mpc to the cluster center (see

Figure 1a). If instead the dispersion is as great as 0.4 mag, then the scale length is  $3.0 \pm 0.5$  Mpc (see Figure 1b). It is unlikely that the intrinsic scatter is greater than 0.4 mag, so the probable value of the scale length lies in the range 2.5-4.0 Mpc. As can be seen, even after deconvolving the data there remains considerable uncertainty in the depth profile of the cluster. This is one of the sources of uncertainty in calculating the Malmquist correction to the cluster distance.

To summarize, the assumed model for the space density of spiral galaxies within Virgo in cluster-centric coordinates is

$$\rho(r, \phi) = e^{-r/l(\phi)}, \quad (6)$$

where  $l(\phi)$  is defined by the expression

$$l(\phi) = \frac{a}{\sqrt{1 - e^2 \cos(\phi)^2}}. \quad (7)$$

Here  $\phi$  is the azimuthal angle of the cluster coordinate system, and  $e$  is the eccentricity of the ellipsoidal model of the cluster. The angle  $\phi$  is defined such that  $\phi = 0$  along the line of sight on the near side of the cluster and  $\phi = \pi$  along the line of sight on the far side. The eccentricity is defined in equation (5), where  $b$  is the line of sight scale length and  $a$  is the scale length projected on the sky. In terms of observables,  $a = r_c \tan(\theta)$ , where  $r_c$  is the distance from us to the center of the cluster, and  $\theta$  is the angular scale length projected on the sky. Current information on the structure indicates  $b = 2.5 - 4.0$  Mpc, and  $\theta = 3.3^\circ$ . For  $r_c \approx 17$  Mpc, this would imply  $a \approx 1.0$  Mpc and  $\frac{b}{a} \approx 2.5 - 4$ , a ratio similar to that of an E6 or E7 elliptical galaxy.

### 3.2. The Parent Distribution of Virgo-like Clusters

The second key issue is the parent distribution of clusters from which Virgo was drawn. It appears that Virgo was chosen by the Key Project because it is the nearest large cluster to the Milky Way. Clearly, only one cluster has that status, and it has exactly one distance, not a distribution of distances. Nevertheless, there is a probability distribution of potential distances from which the real distance was drawn. This is the relevant  $r^2 n(r)$  in equation (2).

To model  $n(r)$ , we consider an ensemble of statistically identical universes<sup>1</sup>. For simplicity, we assume that the populations of Milky Way-like galaxies and large clusters are independently distributed at random with no mutual correlation. We also assume that the distribution of clusters is isotropic. If we place ourselves in any one Milky Way, the distribution  $n(r)$  then depends only on the mean number density of large clusters, assuming that the average density is independent of  $r$ . If that density is high, the nearest cluster will be close by, and  $n(r)$  will peak at a low value of  $r$ . If that density is low, the nearest cluster will be distant, and  $n(r)$  will peak far away. Analytically,

---

<sup>1</sup> Alternatively, we could consider all pairs in our universe of Milky Way-like galaxies and their nearest large clusters.

this function can be derived using Poisson statistics. This yields

$$r^2 n(r) = 4\pi r^2 n_0 e^{-4\pi r^3 n_0/3}, \quad (8)$$

where  $n_0$  is the average cluster density.

The next question is: what is the density of clusters in the universe? More specifically, what is the density of clusters which are at least as rich as Virgo<sup>2</sup>? This question turns out to have a non-trivial effect on the magnitude of the bias. Scaramella et al. carried out a detailed study of the Abell and ACO cluster catalogs (Scaramella et al. 1991). After correcting for selection effects, they determined that the density of clusters of richness class 0 or greater was  $n_0 = 1.46 \pm 0.12 \times 10^{-5} h^3 \text{ Mpc}^{-3}$  for the Abell catalog and  $n_0 = 2.35 \pm 0.15 \times 10^{-5} h^3 \text{ Mpc}^{-3}$  for the ACO catalog. The difference in these two numbers is attributed to several factors, including greater completeness of the ACO catalog, more spurious detections in the ACO catalog due to a different method of cluster detection, and potentially real effects since the two catalogs sample different regions of the sky. Although these density values differ by roughly 60%, they do provide a rough range within which the true density of Abell type clusters likely lies.

Virgo is not an Abell or ACO cluster, but it is generally believed to be comparable to Abell clusters of richness class 0 (Heckman 1981; Vigroux, Boulade, & Rose 1989). Consequently, the Abell and ACO densities can serve as reasonable estimates of the density of clusters of Virgo richness or greater in the local universe.

### 3.3. Further Constraints from Velocity Information

The previous two sections describe the basic geometrical situation which must be modelled. However, we also have velocity information which should be utilized to make modelling of the bias more realistic.

In the basic model, it is assumed that the nearest cluster can lie at any distance, subject to a given probability distribution. The only constraint on the resulting bias is that the observed distance conform to the distance measured to M100. In reality, the simulated clusters must also conform to velocity data available for the cluster and M100.

First consider the velocity of the Virgo cluster. If we have some *a priori* knowledge of the possible range of values for  $H_0$ , then the velocity of the cluster should be used to restrict the range of distances at which the cluster may lie. There appears to be some consensus in the literature that the value of  $H_0$  lies in the range  $90 > H_0 > 50 \text{ km s}^{-1} \text{ Mpc}^{-1}$  (Kennicutt, Freedman, & Mould 1995). Also, the recessional velocity of Virgo relative to the Local Group is  $1396 \pm 96 \text{ km s}^{-1}$  (Huchra 1995). Taking  $1300 < v_{Virgo} < 1500 \text{ km s}^{-1}$  and  $90 > H_0 > 50 \text{ km s}^{-1} \text{ Mpc}^{-1}$ , we

---

<sup>2</sup>We assume that the Key Project would have been content to select any cluster as rich or richer than Virgo.

can roughly restrict  $r$ , the true distance to the center of the Virgo cluster, to be  $14.4 < r < 30$  Mpc. This restriction has very little effect at the upper end of possible cluster distances, but the constraint that  $r > 14.4$  Mpc excludes a significant fraction of candidate clusters (see Figure 2). Consequently, the bias is greater here than in the basic model.

Further, an attempt can be made to utilize information on the velocity of M100 relative to the cluster to constrain its distance relative to Virgo's. Yasuda et al. plot heliocentric velocity versus Tully-Fisher distance for spirals in Virgo (Yasuda, Fukugita, & Okamura 1996). In this plot, very little correlation is seen between these parameters due to virialization of the core. However, no spiral galaxy with a heliocentric velocity greater than  $1000 \text{ km s}^{-1}$  is observed at a Tully-Fisher distance less than 10 Mpc. M100 has a heliocentric velocity of  $1580 \text{ km s}^{-1}$ . It was noted previously that the best deconvolution of this data set gives a Tully-Fisher distance of 14.4 Mpc to the center of the cluster. We can conservatively use this information to place a bound on the ratio of the distance to M100 relative to the distance to the center of Virgo. Specifically, this information implies that  $d_{M100} > \frac{2}{3}d_{Virgo}$ .

## 4. Monte Carlo Simulations

### 4.1. Method

Given the above information on Virgo, a Monte Carlo routine was constructed to numerically evaluate the Malmquist bias in the distance to the cluster center. The center of the cluster was defined to be the peak of the cluster's spiral density distribution.

The logic behind the routine was as follows: First a true distance to the center of a cluster was picked at random based on the assumptions regarding the distribution of Virgo-like clusters. Next a galaxy within the cluster was selected at random based on the assumed distribution of spirals in the cluster, as given in equation (6). The distance to this galaxy,  $r_g$ , was then calculated and a Gaussianly distributed magnitude error was added corresponding to the measurement error in the actual observation. This gave a measured, raw distance,  $d_o$ . If  $d_o$  was equal to the Key Project distance of 16.1 Mpc to within 0.5 Mpc and the galaxy was at a projected separation of less than 6 degrees from the center of the cluster, then the datum was considered consistent. If consistent, the measured distance,  $d_o$ , and actual distance to the cluster center,  $r_c$ , were kept. Otherwise the trial was thrown out. This procedure was repeated until a set number of successful iterations, typically 20,000, were completed.

The Malmquist bias to the cluster was then computed. If  $R$  is defined to be the unbiased true distance to the cluster, then  $R = (\Sigma r_{c,i})/N$ , where  $N$  is the number of trials. Likewise, the mean measured distance to the cluster is  $D_o = (\Sigma d_{o,i})/N$ . The true distance is related to the observed distance by the equation

$$R = (1 + B)D_o, \quad (9)$$

where  $B$  is the Malmquist bias. Rewriting this equation in the form

$$B = \frac{R}{D_o} - 1, \quad (10)$$

the bias can be readily calculated.

## 4.2. Simulations

Simulation of the bias was approached in three stages in order to illustrate the effect of each additional level of information. First, simulations were run for the basic model, ignoring velocity data. Next velocity information for the cluster was included, effectively modifying  $n(r)$ , and in the third stage the velocity information for M100 was used to further constrain  $P(r|D)$ .

As mentioned, uncertainty exists regarding the line of sight distribution of spirals in the cluster. With reasonable confidence it can be assumed that the effective line of sight scale length,  $b$ , of the cluster is between 2.5 and 4.0 Mpc. Monte Carlo simulations were run for a range of scale lengths, and for both Abell and ACO densities. The velocity of Virgo was taken to be 1,396 km s<sup>-1</sup>.

A plot of the underlying cluster probability distribution and the distribution of clusters which satisfied the selection criteria is shown for all three models in Figure 2.

### 4.2.1. Basic Model

Results for the basic model can be seen in Table 1 and Figure 3. That the bias increases with increasing  $b$  is intuitively plausible. Larger  $b$  increases the cluster depth along the line of sight, and thus the relative uncertainty in the distance to the cluster as determined by M100. This may be thought of as an additional error, and hence the bias increases. That the bias approaches a constant value for large scale lengths is less intuitive. This is due to the behavior of  $n(r)$ . Remember that Virgo is the nearest cluster. For large  $r$ , the probability that a cluster at distance  $r$  is the nearest decreases rapidly. Consequently, although increasing  $b$  allows clusters farther away to appear closer, at large  $r$  the parent population  $n(r)$  permits only a negligible contribution to the bias. Least intuitive is that the magnitude of the bias peaks before declining to a constant value for larger scale lengths. This effect is associated with  $n(r)$ . The magnitude of the bias decreases once the scale length is great enough to allow significant sampling of the region beyond the peak of  $r^2 n(r)$ .

For comparison, simulations were also run in which any cluster within 120 Mpc could be Virgo, regardless of whether it was the nearest cluster, as long as the simulation produced an observed distance of  $16.1 \pm 0.5$  Mpc. This corresponds to the low density limit of the nearest cluster case. In the low density case, the magnitude of the bias is greater and varies more with

scale length. Note also that here the bias does not decline or approach a constant value for large  $b$ , but rather continues to increase (Figure 3(a)).

#### 4.2.2. Basic Model + Virgo Velocity Information

These simulations include the constraint  $50 < H_0 < 90 \text{ km s}^{-1} \text{ Mpc}^{-1}$ . The results can be seen in Table 1 and Figure 3(b). It should be noted that the magnitude of the bias is quite sensitive to exactly where the high  $H_0$  cutoff is made. For example, for  $b = 3.0$  and ACO density, changing the minimum allowed distance from 14.4 to 13.7 (i.e. changing the maximum  $H_0$  from 90 to 95) lowers the bias from 7.5% to 6.4%. For plausible scenarios with  $d_{cutoff} = 14.4$ , this model yields a bias of 7.4-8.3%.

#### 4.2.3. Full Model

This adds the second constraint that  $d_{Virgo} < \frac{3}{2}d_{M100}$ . The results can be seen in Table 1 and Figure 3(c). The form of the bias as a function of scale length is very similar to the previous model, only with a smaller bias. The primary difference is that the bias decreases more rapidly now with increasing  $b$  since a greater fraction of distant clusters are now excluded. Plausible parameters now yield a bias of 6.5-7.6%.

## 5. Discussion

We have shown that, with present data, Malmquist bias noticeably alters the most probable distance to the Virgo cluster. Unfortunately, it is not possible to determine the precise magnitude of the bias. In the basic model, this is due to two key uncertainties: i) uncertainty in the spiral galaxy depth profile in the cluster, and ii) uncertainty as to the density and distribution of clusters. Of the two, the second leads to a greater uncertainty in the bias. In the models which include velocity information, it is seen that additional information regarding the cluster changes  $n(r)$  and  $P(r|D)$  and hence the magnitude of the bias. This additional knowledge leads to a more realistic estimation of the bias; however, it also contributes uncertainty in the magnitude of the bias since this knowledge is incomplete.

Given present knowledge, the magnitude of the bias is likely 6.5-8.5%. For a raw distance of 16.1 Mpc, this implies an unbiased true distance of 17.2 to 17.4 Mpc.  $H_0$  likewise decreases from a raw value of  $87 \text{ km s}^{-1} \text{ Mpc}^{-1}$  to an unbiased value of  $80-82 \text{ km s}^{-1} \text{ Mpc}^{-1}$ . In particular, if the density of clusters is taken to be comparable to the ACO density in the full model, with  $b = 3.5$  Mpc, this yields  $d = 17.2 \pm 1.9$  Mpc and  $H_0 = 81 \pm 11 \text{ km s}^{-1} \text{ Mpc}^{-1}$ . This is one of the scenarios most consistent with the data, assuming that the intrinsic dispersion of the TF relation for Virgo

is comparable to that of field galaxies. Finally, it should be realized that the bias computed here includes only the bias associated directly with the Cepheid-based determination of the distance to the Virgo cluster. In fact, the calibration of the Cepheid P-L relation is dependent on the distance to the Large Magellanic Cloud. Bias in the distance to the LMC would lead to additional bias in the distance to Virgo. The effect of this bias has not been included in this paper.

## 6. Conclusions

The Malmquist bias associated with the  $H_0$  Key Project determination of the distance to the Virgo cluster is of order 6-8%, which is significant. However, this particular bias correction is only of temporary interest, as Virgo will soon cease to be the lynchpin of the Key Project. Of more lasting interest, this exercise serves to illustrate several general issues which often arise when considering the effect of Malmquist bias on astronomical distance measurements.

One issue is the subtle effect on the bias of exactly how an object is defined. The definition of the object defines the parent population from which the object is drawn,  $n(r)$ , and hence changes the bias. In the case of Virgo, there is a clear change in the bias resulting from changing the parent population from *all* large clusters to the *nearest* large cluster<sup>3</sup>. Similarly, the exact bias is sensitive to the spatial model of the cluster,  $\rho(r, \phi)$ . The extended nature of the cluster introduces uncertainty which contributes to the bias in the same fashion as other observational errors. The more extended the cluster is along the line of sight, the greater the bias.

Another important fact illustrated here is that Malmquist bias is present when the distance to a single object is measured. Most published astronomical distances are to single objects. They are essentially *all* biased, most in such a way that the measured distance is *too small*. This is as true for parallax measurements to stars as for extragalactic measurements<sup>4</sup> (Lutz and Kelker 1973; Hanson 1979).

The implications of this are particularly important with regard to “distance ladders”. With each additional step in such a ladder, the total uncertainty increases. For instance, for Gaussian magnitude errors, the uncertainty increases in quadrature as  $\sigma_{tot}^2 = \Sigma \sigma_i^2$ . Thus, for the simple case of constant  $n(r)$  and  $\sigma_i$ , the bias increases linearly with the number of steps (Equation 4). In light of this fact, it is clearly important to minimize the number of steps, and to treat properly any bias in those steps that are retained.

---

<sup>3</sup>Note that even this treatment of  $n(r)$  falls short because it does not include a probable positive statistical correlation between the Milky Way and Virgo-like clusters due to the galaxy-cluster correlation function. However, our aim is to be illustrative rather than exact, so we have omitted this.

<sup>4</sup>In the field of astrometry this bias is referred to as the Lutz-Kelker effect, and is generally of much greater magnitude than in our present case.

## 7. Acknowledgments

AG would like to thank everyone in the office for letting him bounce ideas off of them. He also acknowledges the NSF for support of this work under a Graduate Research Fellowship. SF would like to thank Jeff Willick and Avishai Dekel for their discussions regarding Malmquist bias. We both wish to thank the anonymous referee for the excellent suggestion that we include velocity constraints in the models.

Table 1. Results of Monte Carlo simulations.

$b$	$B$	$d_{Virgo}$	$H_0$	$B$	$d_{Virgo}$	$H_0$
Abell Density						
Basic Model				ACO Density		
2.5	5.5	$17.0 \pm 2.5$	$82 \pm 13$	4.4	$16.8 \pm 2.4$	$83 \pm 13$
3.0	5.4	$17.0 \pm 2.6$	$82 \pm 14$	4.6	$16.8 \pm 2.4$	$83 \pm 13$
3.5	5.4	$17.0 \pm 2.6$	$82 \pm 14$	4.5	$16.8 \pm 2.5$	$83 \pm 14$
4.0	5.5	$17.0 \pm 2.7$	$82 \pm 14$	4.5	$16.8 \pm 2.4$	$83 \pm 13$
Basic Model plus $H_0$ Cutoff						
2.5	8.3	$17.4 \pm 2.2$	$80 \pm 12$	7.6	$17.3 \pm 2.1$	$81 \pm 11$
3.0	8.2	$17.4 \pm 2.3$	$80 \pm 12$	7.5	$17.3 \pm 2.1$	$81 \pm 11$
3.5	8.1	$17.4 \pm 2.3$	$80 \pm 12$	7.4	$17.3 \pm 2.1$	$81 \pm 11$
4.0	7.9	$17.4 \pm 2.2$	$80 \pm 12$	7.4	$17.3 \pm 2.1$	$81 \pm 11$
Full Model						
2.5	7.6	$17.3 \pm 2.0$	$81 \pm 11$	7.2	$17.3 \pm 1.9$	$81 \pm 10$
3.0	7.4	$17.3 \pm 2.0$	$81 \pm 11$	7.0	$17.2 \pm 1.9$	$81 \pm 11$
3.5	7.3	$17.3 \pm 2.0$	$81 \pm 11$	6.8	$17.2 \pm 1.9$	$81 \pm 11$
4.0	7.0	$17.2 \pm 1.9$	$81 \pm 11$	6.6	$17.2 \pm 1.8$	$81 \pm 10$

Note. —  $b$ : Line of sight scale length(Mpc),  $B$ : Malmquist bias(%),  $d_{Virgo}$ : Bias-corrected Distance to Virgo(Mpc),  $H_0$ : Bias-corrected  $H_0$ (km s<sup>-1</sup> Mpc<sup>-1</sup>)

Table 2. Key Project and Malmquist corrected data.

	Key Project Value	Abell Density Corrected Value	ACO Density Corrected Value
Virgo Recessional Velocity	$1396 \pm 96 \text{ km s}^{-1}$	...	...
Distance to M100	$16.1 \pm 1.3 \text{ Mpc}$	...	...
Distance to Virgo	$16.1 \pm 3.5 \text{ Mpc}$	$17.3 \pm 2.0$	$17.2 \pm 1.9$
$H_0$	$87 \pm 20 \text{ km s}^{-1} \text{ Mpc}^{-1}$	$81 \pm 11$	$81 \pm 11$

Note. — The error in the Key Project distance to Virgo corresponds to a 20% Gaussian uncertainty added in quadrature to the uncertainty in the distance to M100. Also, the value of  $H_0$  in the Key Project column is not directly from Ferrarese et al. Rather, it was calculated here from the information given in that paper.

## REFERENCES

Bachall, N.A., Annual Reviews of Astronomy and Astrophysics, 26, 631

Binggeli, B., Sandage, A., & Tammann, G. 1985, AJ, 90, 1681

Binggeli, B., Sandage, A., & Tammann, G. 1987, AJ, 94, 251

Ferrarese, L., et al. 1996, ApJ, 464, 568

Foquè, P., Bottinelli, L., Gougenheim, L., & Paturel, G. 1990, ApJ, 349, 1

Freedman, W., et al. 1994, Nature, 371, 757

Fukugita, M., Okamura, S., & Yasuda, N. 1993, ApJ, 412, L13

Hanson, R. 1979, MNRAS, 186, 875

Heckman, T.M. 1981, ApJ, 250, L59

Huchra, J.P. 1995, The MSSSO Heron Island Workshop on Peculiar Velocities in the Universe,  
<http://msowww.anu.edu.au/~heron/Huchra/huchra.html>

Kennicutt, R., Freedman, W., & Mould, J. 1995, AJ, 100, 1475

Landy, S., & Szalay A. 1992, ApJ, 391, 494

Lutz, T., & Kelker, D. 1973, PASP, 85, 573

Lynden-Bell, D., et al. 1988, ApJ, 326, 19

Mould, J., et al. 1995, ApJ, 449, 413

Malmquist, K.G. 1924, Medd. Lund Astron. Obs., Ser. II, No. 32, 64

Pierce, M., & Tully, R. 1988, ApJ, 330, 579

Sandage, A., Binggeli, B., & Tammann, G. 1985, in The Virgo Cluster, ed. O. Richter & B. Binggeli (Garching:ESO), 181

Scaramella, R., Zamorani, G., Vettolani, G., Chincarini, G., AJ, 101, 342

Strauss, M., & Willick, J. 1995, Physics Reports, 261, 271

Tully, R., & Shaya, E. 1984, ApJ, 281, 31

Vigroux, L., Boulade, O., Rose, J. A. 1989, AJ, 98, 2044

Willick, J. 1991, PhD. thesis, University of California, Berkeley

Yasuda, N., Fukugita, M., & Okamura, S. 1996, submitted to ApJ

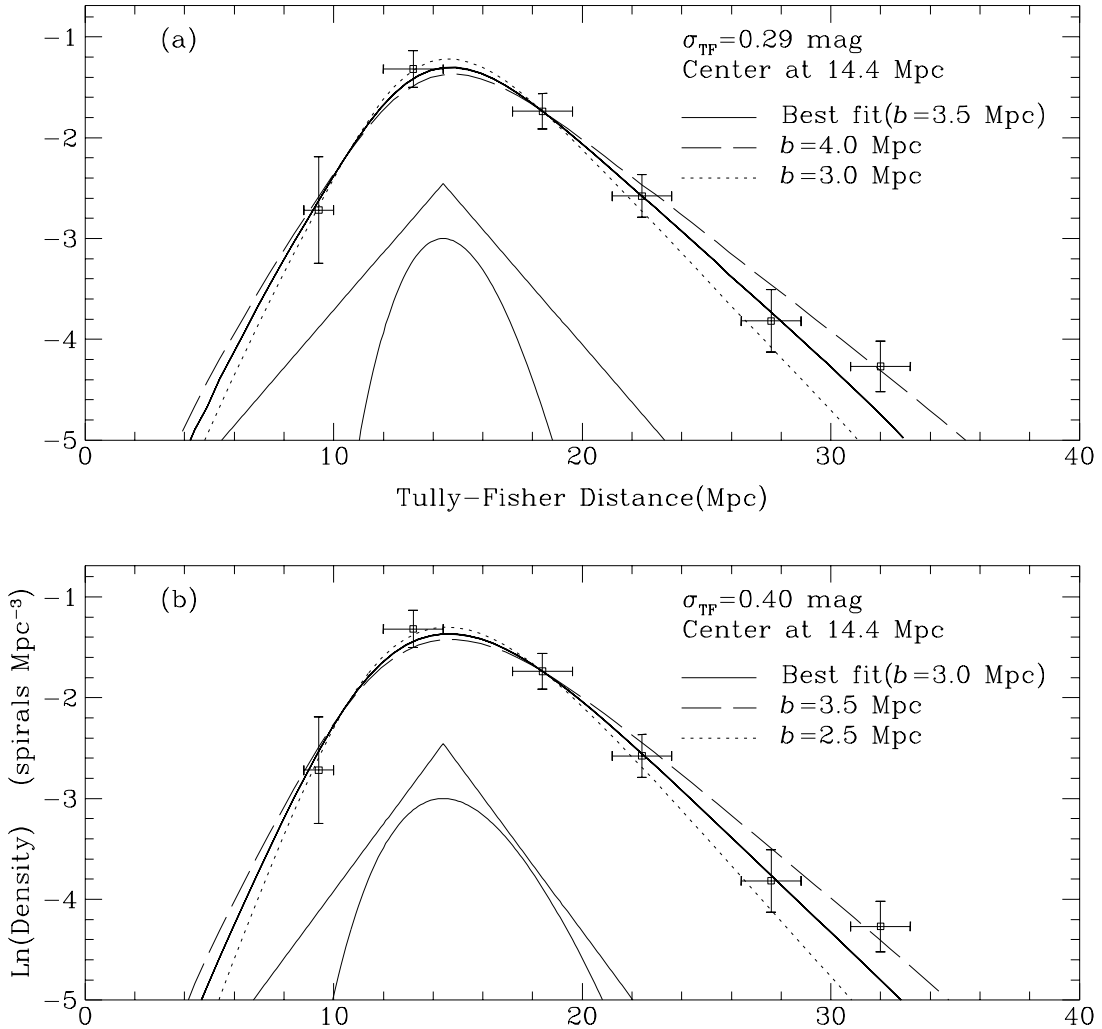


Fig. 1.— Two models for the spatial density of spiral galaxies towards Virgo as a function of raw TF distance (Fukugita et al 1993). The heavy solid curves are the best fit cases. The dashed and dotted curves are for values of  $b$  which are 0.5 Mpc greater or less than the best fit, respectively. The two solid curves beneath the fit show the form of the intrinsic distribution and Gaussian magnitude error which were convolved.

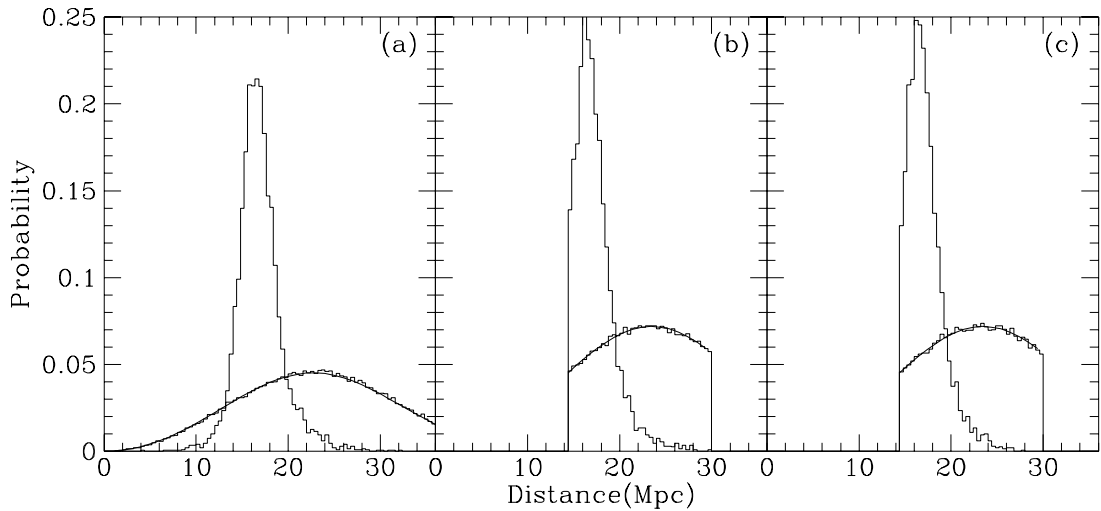


Fig. 2.— The lower histogram in each frame shows the distribution of distances to the nearest cluster in the Monte Carlo simulations. The solid curve beneath it is the analytic function for this distribution. The upper histogram is the distribution of distances to the nearest cluster which produced the observed distance to M100 in the simulations for ACO density,  $b=3.0$ . Figures 2(a), 2(b), and 2(c) are for the basic model, basic model plus  $H_0$  cutoff, and full model, respectively. All curves are normalized to unit probability.

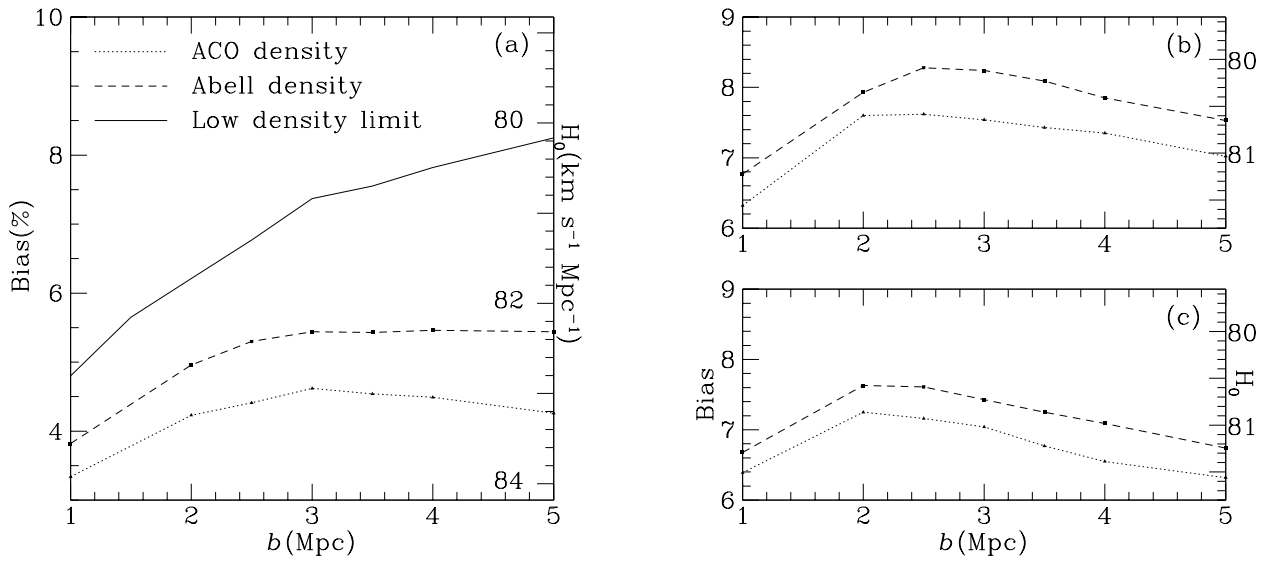


Fig. 3.— Bias as a function of the depth profile of Virgo for Abell and ACO density. For the basic model, the low density limiting case is also shown. Figures 3(a), 3(b), and 3(c) are for the basic model, basic model plus  $H_0$  cutoff, and full model, respectively.